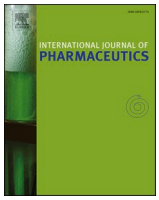
International Journal of Pharmaceutics 666 (2024) 124809



Contents lists available at ScienceDirect

International Journal of Pharmaceutics

journal homepage: www.elsevier.com/locate/ijpharm





Nano-strategies for advancing oral drug delivery: Porous silicon particles and cyclodextrin encapsulation for enhanced dissolution of poorly soluble drugs

Hennie Marie Johnsen [a,b,*], Werner Filtvedt [b], Jo Klaveness [a], Marianne Hiorth [a]

[a] Department of Pharmacy, University of Oslo. Sem Sælands vei 3, 0371 Oslo, Norway
[b] Nacamed AS. Oslo Science Park, Gaustadalléen 21, 0349 Oslo, Norway

ARTICLE INFO

Keywords:
Oral Drug Delivery
Nanoparticles
Silicon nanoparticles
Cyclodextrin
Dissolution enhancement
Poorly soluble drugs
BCS class II

ABSTRACT

Development of novel active pharmaceutical ingredients (API) for oral use often face challenges due to low bioavailability. Nanoparticle-based drug delivery systems and cyclodextrin (CD) encapsulation offer promising solutions by enhancing API solubility or dissolution rates. Porous silicon nanoparticles have shown potential to encapsulate APIs in their amorphous form within the pores, improving their dissolution rates compared to crystalline counterparts. A novel synthesis approach, circumventing the expensive and tedious synthesis from Si wafer material, has been developed using centrifugal Chemical Vapor Deposition (cCVD). Herein, various cCVD Si particles were evaluated for their ability to enhance the dissolution rate of the model drugs celecoxib (CEL), phenytoin (PHT), griseofulvin (GRI), diclofenac (DCF) and naproxen (NAP). Our findings demonstrate increased dissolution rates of all tested APIs when formulated with cCVD Si particles, compared to free API in pH 7.4 or pH 2.0. Particle characteristics were largely retained after loading, and the solid state of the loaded APIs were evaluated using Differential Scanning Calorimetry (DSC). Dissolution kinetics were influenced by the particle properties, mass loading and API characteristics. Loading of CD-CEL, −GRI and −DCF complexes into the cCVD Si particles showed a potential for further enhanced dissolution rates, representing the first reported investigation of this combination. In conclusion, the cCVD Si particles are promising for improving the dissolution rate of poorly soluble drugs, potentially due to precipitation of amorphous or metastable forms. Further enhancements were observed upon loading CD-drug complexes, thereby offering promising strategies for optimizing drug bioavailability.

1. Introduction

Poor bioavailability is one of the major challenges when developing new Active Pharmaceutical Ingredients (API) intended for oral administration. Oral delivery remains the preferred route for routine, non-invasive patient care. Yet, a major challenge lies in this convenience: limited bioavailability is often a problem with over 40 % of API under development failing in clinical trials due to suboptimal pharmacokinetic profiles (Sun et al., 2022). Inadequate oral bioavailability can be caused by either low aqueous solubility of the API within the gastrointestinal tract or poor penetration though the intestinal walls once in solution. Classifying drugs under the Biopharmaceutics Classification System (BCS) sheds light on the underlying causes based on these two factors. Class II compounds possess sufficient permeation characteristics but are hampered by low intrinsic solubility and/or dissolution rates (Samineni et al., 2022). It has been claimed that up to 90 % of pipeline APIs and 40 % of marketed drugs suffer from poor solubility based on the BCS (Loftsson and Brewster, 2010; GlobalData Healthcare, 2018). In response, several pharmaceutical formulation strategies have been developed to improve the dissolution and bioavailability of the BCS class II type of drugs. This includes self-emulsifying drug delivery systems, amorphous solid dispersions, nanocrystal formation or encapsulation into cyclodextrin complexes or nanosized drug carriers (Fahr and Liu, 2007). Technological limitations set restrictions for the type of APIs that are suitable for each formulation strategy and development of novel versatile strategies is vital to cover the needs of the wide range of API characteristics.

Various types of nanomaterials have emerged as potential carriers for

* Corresponding author at: Department of Pharmacy, University of Oslo. Sem Sælands vei 3, 0371 Oslo, Norway.
E-mail address: h.m.johnsen@farmasi.uio.no (H.M. Johnsen).

https://doi.org/10.1016/j.ijpharm.2024.124809
Received 14 May 2024; Received in revised form 4 October 2024; Accepted 5 October 2024
Available online 9 October 2024
0378-5173/© 2024 The Author(s). Published by Elsevier B.V. This is an open access article under the CC BY license (http://creativecommons.org/licenses/by/4.0/).

improving drug solubility. This includes organic materials like polymers, liposomes and micelles, and inorganic materials like gold, carbon, silica and silicon. Inorganic materials can offer advantages due to their solid nature and the possibility to possess porous structures capable of encapsulating drugs in their amorphous state due to spatial confinement that restricts crystal growth of the loaded drug. Amorphous form of drugs can be used to promote faster dissolution compared to their stable crystalline counterparts. This concept has been explored using porous silicon nanoparticles fabricated through electrochemical HF etching of wafer material. Studies employing this material have shown enhanced dissolution rates for multiple drugs, often accompanied by characterization of non-crystalline drug forms (Wang et al., 2014; Riikonen et al., 2015; Wang et al., 2010; Salonen et al., 2005; Lehto et al., 2013). For example, enhanced *in vitro* dissolution rates of the BCS class II drugs celecoxib (Wang et al., 2014; Riikonen et al., 2015) and indomethacin (Wang et al., 2010) have been demonstrated, accompanied by characterizations of the non-crystalline drug form loaded within HF-etched silicon particles. Another study investigating five drugs loaded into similar particles demonstrated improved release profiles for poorly soluble drugs and a delayed response for more soluble drugs, with an overall reduction in pH dependent release (Salonen et al., 2005). However, the tedious and toxic HF etching process for synthesis of porous Si nanoparticles is suffering from low yields (Lee et al., 2024). A novel scalable one-step synthesis route that eliminates these setbacks, known as Centrifugal Chemical Vapor Deposition (cCVD), has been investigated for fabrication of drug delivery materials with promising results. The cCVD Si particles comprise of multiple solid particles packed together in a stable aggregate form, allowing for loading of drugs within the porous structure between the primary particles (Johnsen et al., 2024).

Another commonly used strategy for enhancing the performance of BCS class II drugs involves the formation of drug inclusion complexes with cyclic oligosaccharide molecules, namely cyclodextrins (CD). Upon complexation, the drug is entrapped within the lipophilic inner cavity of the CD ring structure and improved solubility is attributed to the hydrophilic outer part (Jacob and Nair, 2018). Some CDs are categorized as GRAS (generally recognized as safe) by the American Food and Drug Administration (FDA) and are used in several industries including food, cosmetics, chemicals and pharmaceuticals. Notably, the βCD derivatives (β for seven glucose units) 2-hydroxypropyl-βCD (HPCD) and sulfobutylether-βCD (SBCD) are non-toxic and have been approved for both oral and parenteral use. The combination of CDs and nanocarriers has been studied for organic nanoparticles including liposomes, niosomes, micelles, polymeric and solid-lipid nanoparticles, with promising outcomes in improving effectiveness compared to the individual strategies (Mura, 2020). However, the potential synergistic dissolution effects of combining CD-drug inclusion complexes with silicon-based nanocarriers have to the best of the authors' knowledge not been investigated in existing literature.

The primary objective of this study was to assess the suitability of cCVD Si nanoparticles in enhancing the dissolution rate of five BCS class II model drugs: celecoxib, phenytoin, griseofulvin, diclofenac, and naproxen. These drugs were selected due to their chemical properties such as low solubilities covering both ionic (acidic drugs) and neutral drugs, in the release mediums studied, to examine effects of ionization. Their poor or variable oral bioavailability could benefit from improved dissolution. Additionally, we aimed to investigate how loading HPCD- and SBCD-drug complexes into cCVD Si particles influences release properties and to explore the effects of Si particles' surface area and mass loading.

2. Materials and methods

2.1. Materials

Celecoxib (CEL) was gifted from Drug Discovery Laboratory AS and phenytoin (PHT) from Kragero Tablettproduksjon AS. Griseofulvin (GRI) was obtained from Sigma, and diclofenac (DCF) and naproxen (NAP) from Merck. Table 1 lists the chemical properties of the chosen drug substances. (2-Hydroxypropyl)-β-cyclodextrin (HPCD) was purchased from Sigma-Aldrich, β-Cyclodextrin sulfobutyl ether sodium salt (SBCD) from Biosynth Carbosynth and rectified ethanol from Antibac AS. Hydrochloric acid (HCl), HPLC grade water and acetic acid were purchased from Merck. Acetonitrile and PBS tablets were purchased from Sigma-Aldrich.

The porous cCVD Si particles were provided from Dynatec Engineering AS and were produced from thermal decomposition of silane gas (SiH_4) in a centrifugal Chemical Vapor Deposition reactor as previously described (Johnsen et al., 2024; Johnsen et al., 2022). The reactor parameters were adjusted to grow stable "snow lantern" aggregated particles by maximizing the formation of large numbers of nuclei, many particle-to-particle collisions and enhancing the tendency for particles to adhere to each other. Two different particles were used for this study (Si1 and Si2), with different particle sizes and surface area, controlled by adjusting the reactor parameters including gas flow, concentration, growth time in the reactor and centrifugal force. The Si1 particles consisted of pure Si (from SiH_4 decomposition) and the Si2 particles contained a small amount of carbon homogenously distributed in the Si matrix, prepared by addition of a carbon-containing gas in the cCVD process (Kirkengen et al., 2021).

2.2. Cyclodextrin complexation and loading of API and CD-API into cCVD Si particles

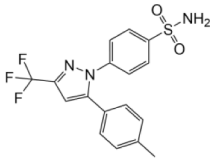
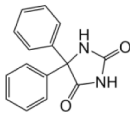
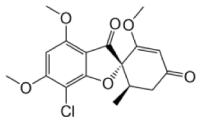
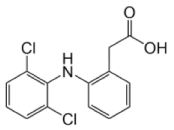
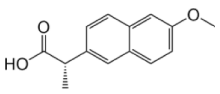
Complexation between CDs and CEL, GRI or DCF was performed by mixing 1:1 (mol ratio) of the drug (5–20 mg) and β-cyclodextrin, HPCD or SBCD, with a manual Eppendorf homogenizer. The powders were then dissolved in 1–1.5 ml of 1:1 H_2O:EtOH and placed in an ultrasonicator bath for 5 min before drying under vacuum. All vacuum drying was done at room temperature (22 °C) overnight in a Memmert Universal oven connected to a vacuum pump providing full vacuum (<5 mbar). All as-prepared samples were stored in refrigerator after drying and used for experiments within two weeks. NAP and PHT were not chosen for CD complexation as loading with Si particles was regarded as sufficient for improving their dissolution rates.

Loading of the drugs alone, CEL, PHT, GRI, DCF and NAP, or drug-CD complexes, HPCD- and SBCD-CEL, −GRI and −NAP, into the Si particles was performed by the impregnation loading technique. This procedure, exemplified by loading of CD-GRI complexes into cCVD Si particles, is illustrated in Fig. 1. First, the drug or drug-CD was dissolved in ethanol (96 %). Then, the drug-comprising solution was mixed with Si particles (Si1 or Si2) before the dispersion was placed in an ultrasonicator bath for 10 min followed by drying the ethanol under vacuum at room temperature overnight. The free drug substances were treated the same way, but without addition of particles. Different mass load (mass of loaded drug/mass of drug loaded particles) of 5 % and 20 % were made by adjusting the weight of particles and the drugs. 5 % drug load was used for all the CD-API loaded particles. Physical mixtures were made, for DSC reference, by thoroughly homogenizing dry powder of drug and particles with a spatula. The API loaded formulations are named as follows: SiX-Y%-API, where X is either 1 or 2 for Si1 and Si2 and Y is either 5 or 20 corresponding to the loading %. Physical mixture samples are called Mix Y%-API and the loaded CD complexes (loaded in Si1) are named Si1-HPCD-API and Si1-SBCD-API.

2.3. Particle and API characterization

Particle size and surface charge (zeta potential) characterizations of the un-loaded and loaded particles were performed by Dynamic Light Scattering (DLS) using the Zetasizer Nano ZS (ZEN3600, Malvern instruments) and the Zetasizer software (version 8.01), with detection of backscattered light at an angle of 173° using a red laser (λ = 633 nm).

Table 1
Properties of the model five drugs studied herein. Most data are obtained from Pubchem (unmarked). *Computed logP values (XLogP3 3.0). **Properties estimated in ChemDraw.

Drug	Structure	Chemical formula	Mw (g/mol)	pKa	logP*/**	logS**	PSA** (Å^2)	Aqueous solubility, 25 °C (mg/L)	Melting temp. (°C)	Oral bioavailability
Celecoxib		$C_{17}H_{14}F_3N_3O_2S$	381	11.1 (weak acid)	3.4–4.3	−5.81	75.8	6.1 (Madan et al., 2020)	157–159	22–40 % (Paulson et al., 2001)
Phenytoin		$C_{15}H_{12}N_2O_2$	252	8.3 (acid)	2.1–2.5	−3.49	58.2	32.0	295–298	70–100 % (Inselman and Hansen, 2014)
Griseofulvin		$C_{17}H_{17}ClO_6$	353	–	2.1–2.2	−3.40	71.1	8.6	220	25–70 % (Lin et al., 1973)
Diclofenac		$C_{14}H_{11}Cl_2NO_2$	296	4.2 (acid)	4.1–4.4	−4.71	49.3	2.4–17.8 (Chiarini et al., 1984)	283–285	54–90 % (León-Reyes et al., 2009)
Naproxen		$C_{14}H_{14}O_3$	230	4.2 (acid)	3.0–3.2	−3.01	46.5	15.9	152–155	~100 % (Runkel et al., 1972)

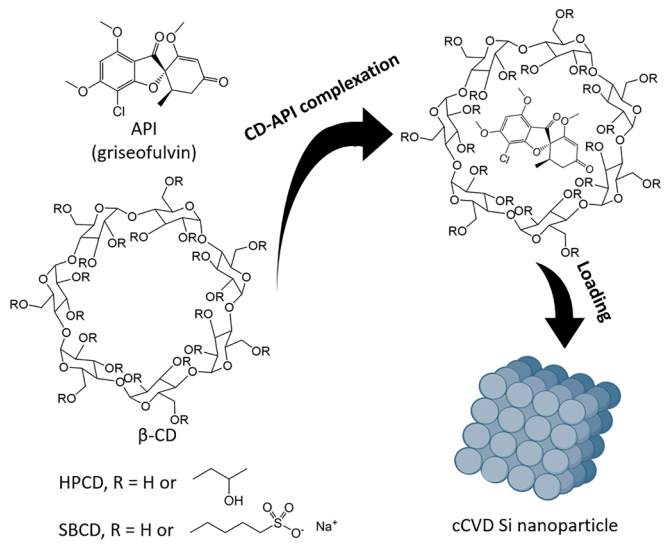


Fig. 1. Illustration of API (griseofulvin shown in this image) complexation with beta-CD with the structures shown. The complex (or the free drug) was then loaded into the cCVD Si particles.

The particles were dispersed to a concentration of 10–50 μg/ml in purified water and ultrasonicated for 1 min before measuring the hydrodynamic diameter as the average of 3 measurements and electrophoretic mobility (Smoluchowski approximation) as the average of 5 measurements, using a standard disposable and zeta potential cuvette, respectively.

Brunauer-Emmett-Teller (BET) surface area, pore size and volume estimates of the Si particles were done from nitrogen gas adsorption data obtained in a Micromeritics 3Flex instrument (Version 5.01.05, Micromeritics Instrument Corporation) after degassing the samples for 16 h at 300 °C. The BET particle size was calculated as previously described (Johnsen et al., 2024) using the density of Si ρ = 2.329 g/cm^3 and assuming spherical particles.

The carbon content of Si particles was determined by combustion analysis in a Leco CS200 instrument. A sample was fully combusted in a flow of pure oxygen, and the amount of released CO and CO_2 was determined by IR spectroscopy.

The loaded, mixed and free API samples were characterized by Differential Scanning Calorimetry (DSC) using the Mettler Toledo DSC822e instrument and the STARe software (version 13.00, Mettler Toledo) with a heating rate of 10 °C/min and a temperature range suitable for the melting point of each drug substance (see Figures S1-S8).

Water content of the HPCD and SBCD starting materials was measured in triplicates using a coulometric Karl Fischer method with the C20 Coulometric KF Titrator (Mettler Toledo) and CombiCoulomat fritless Karl Fischer reagent (Merck).

2.4. Drug release studies and HPLC analyses

Drug release and dissolution studies were performed in PBS solution pH 7.4 or HCl pH 2.0 (0.01 M). The drug concentrations used were approximately 5 μg/ml for CEL (or 1.4 μg/ml in Figure S9), 10 μg/ml for PHT, 6 μg/ml for GRI, 10 μg/ml for DCF and 12 μg/ml for NAP in pH 7.4, 4 μg/ml for DCF and NAP in pH 2.0. All sample tubes of 50 ml were dipped in an ultrasonicator bath for 3 seconds and gently twisted to disperse the particles and obtain a homogenous dispersion of the particles in the release medium, then they were placed on a rolling board (~50 rpm) and kept at room temperature (~22 °C). Samples of 1.2 ml were withdrawn after 5 min, 15 min, 30 min, 1 h, 2 h, 4 h, 8 h and 24 h and centrifuged at 14 k rpm for 10 min (Jouan A14 Micro Centrifuge) for suspending the particles down to a visible pellet. 0.6 ml taken from the top of the supernatants were analyzed by HPLC for quantification of the

Table 2
Characteristics of the cCVD Si NPs used in this study from DLS, BET and carbon content analyses.

	Si1	Si2
DLS size (Z.av, d., nm)	209.5	182.6
DLS PDI	0.18	0.18
Zeta potential (mV)	−37.3	−41.0
Surface area (m^2/g)	56	89
Pore size ad/de (nm)	11.6/ 12.2	11.6/ 12.0
Pore volume (cm^3/g)	0.17	0.27
BET size (d., nm)	46.9	29.5
Carbon content (weight%)	0	1.6

released drug amount (API or API-CD). An overview of the release studies performed can be found in Table S1.

Reverse-phase HPLC analyses were done for quantification of released/dissolved API by comparing peak integration area at the drug's peak wavelength (252 nm for CEL, 225 nm for PHT, 292 nm for GRI, 276 nm for DCF, 234 nm for NAP) to a standard curve of each drug substance. The Finnigan Surveyor system (Thermo) with Photo-Diode-Array (PDA, 200–400 nm) detection and the Xcalibur software (Thermo) was used for HPLC analyses and batch integration was done using the Genesis algorithm in Quan browser. A PLRP-S column (2.1x5mm, Agilent) was used with a mobile phase consisting of an A phase of HPLC grade water with 0.1 % acetic acid and a B phase of HPLC grade acetonitrile with 0.1 % acetic acid. Isocratic elution with 100 µl/min flow rate was used for all drugs with appropriate amounts of the B phase for each drug (70 % B for CEL and DCF, 60 % B for GRI and NAP and 40 % B for PHT). No degradation of the APIs in the release mediums was observed as only a single peak was present in the chromatograms.

2.5. Statistical analyses

All drug release studies were conducted in three parallels. The average percentage of API released at each time point, the corresponding standard deviations and p-values were calculated using Microsoft Excel (version 2207) assuming a normal distribution and using the student *t*-test. Statistical significance was set at $p < 0.05$.

3. Results and discussion

3.1. Particle characterizations

The characteristics of as-prepared Si1 and Si2 particles without loaded cargo are shown in Table 2. Both types of particles exhibited high surface areas, which resulted in lower BET size estimations than the observed hydrodynamic diameter (DLS size), indicating an aggregated particle structure. The hydrodynamic diameters were about 210 nm and 183 nm, and the primary particle (BET) sizes were about 47 nm and 30 nm, for Si1 and Si2, respectively. These findings align with previous reports on the characteristics of aggregated cCVD particles, and their mesoporous structure render them suitable for drug delivery (Johnsen et al., 2024; Santos et al., 2011). The main difference between the two particles was a higher surface area and pore volume for the Si2 particles compared to Si1, arising from aggregation of smaller primary particles as seen from the BET size. Particles with higher porosity and pore volume can potentially carry a higher drug payload in an amorphous (non-crystalline) state within the pores. Si2 also had a low carbon content of 1.6 %.

Characteristics of the studied formulations, free, Si loaded, CD-complexed and CD-complexed-Si loaded drugs, are shown in Table 3 and Table S2 for both Si1 and Si2 particles. Particle sizes remained in the same range as before loading (± 25 nm) for most formulations. Some formulations displayed a larger particle size, mostly for the Si2 particles, accompanied by increased PDI which might be caused by agglomeration, possibly induced by loading of lipophilic drugs. Some particles had a slightly lower size, particularly for the Si1 particles, without showing signs of disassembly of the aggregate structure into primary particles as only one peak remained visible in the size distribution data. This may have arisen from the differences between the aggregate particles' geometry and the assumptions of homogenously sized solid spherical

Table 3
DLS and DSC characteristics (transition enthalpies and onset/peak temp.) of representative formulations made using Si1, Si2, HPCD, CEL, PHT, GRI, DCF and NAP. N/A indicates no visible/detectable peak. Particle size (z.av), polydispersity index (PDI) and zeta potential (pot.) given as mean ± standard deviation. Characterization data for the remaining formulations (physical mixtures and CD-complexes) can be found in Table S2. *Enthalpy of transition at the indicated temperatures, normalized to the API weight.

Sample	Z.av (d.nm)	PDI	Zeta pot. (mV)	Enthalpy of transition (J/g)*	Onset/ peak temp. (°C)
CEL	–	–	–	55.8	150/ 157
Si1-5 %-CEL	185.7 ± 2.9	0.14 ± 0.03	−43.2 ± 0.6	N/A	N/A
Si1-20 %-CEL	210.1 ± 2.9	0.22 ± 0.05	−43.2 ± 1.4	53.5	146/ 154
Si2-5 %-CEL	194.4 ± 6.8	0.27 ± 0.02	−37.2 ± 1.1	N/A	N/A
Si2-20 %-CEL	233.6 ± 18.2	0.33 ± 0.05	−42.1 ± 0.8	−20.5 & 32.0	95/ 103 & 154/ 160
PHT	–	–	–	133.4	294/ 296
Si1-5 %-PHT	173.9 ± 1.3	0. 15 ± 0.01	−42.4 ± 1.2	54.0	277/ 286
Si1-20 %-PHT	191.3 ± 2.9	0.17 ± 0.01	−44.7 ± 2.0	111.0	290/ 295
Si2-5 %-PHT	187.1 ± 2.3	0.21 ± 0.03	−40.5 ± 1.1	N/A	N/A
Si2-20 %-PHT	189.7 ± 5.0	0.22 ± 0.02	−38.7 ± 0.7	33.5	282/ 288
GRI	–	–	–	114.7	220/ 223
Si1-5 %-GRI	180.9 ± 2.2	0.17 ± 0.03	−42.1 ± 1.0	N/A	N/A
Si1-20 %-GRI	173.2 ± 4.8	0.16 ± 0.02	−47.4 ± 1.2	48.0	205/ 214
Si2-5 %-GRI	186.5 ± 2.1	0.16 ± 0.03	−42.3 ± 0.7	N/A	N/A
Si2-20 %-GRI	176.4 ± 1.9	0.17 ± 0.02	−47.3 ± 0.8	46.5	206/ 217
DCF	–	–	–	154.5	178/ 179
Si1-5 %-DCF	188.2 ± 0.4	0.18 ± 0.02	−46.3 ± 1.0	N/A	N/A
Si1-20 %-DCF	173.1 ± 3.5	0.18 ± 0.02	−46.3 ± 1.1	100.5	156/ 167
Si2-5 %-DCF	255.6 ± 5.6	0.36 ± 0.04	−45.0 ± 1.0	N/A	N/A
Si2-20 %-DCF	215.8 ± 4.8	0.28 ± 0.01	−40.7 ± 0.7	65.5	152/ 163
NAP	–	–	–	153.3	158/ 159
Si1-5 %-NAP	206.5 ± 0.4	0.22 ± 0.02	–33.2 ± 1.2	68.0	123/ 144
Si1-20 %-NAP	189.6 ± 0.7	0.18 ± 0.02	–33.9 ± 2.5	114.0	152/ 157
Si2-5 %-NAP	238.1 ± 13.3	0.28 ± 0.05	−29.6 ± 1.2	N/A	N/A
Si2-20 %-NAP	234.0 ± 5.4	0.31 ± 0.01	−41.1 ± 1.5	99.5	152/ 155

particles in DLS measurements. After loading, the particles have less porosity and might have properties more similar to the assumptions used in DLS measurements, giving a more accurate particle size. The particle charge remained highly negative, below −29 mV, for the loaded particles with slight variations for the different drugs.

DSC curves for all the prepared formulations are shown in Figure S1-S8 for the different drugs. The enthalpy of transition, and the corresponding onset and peak temperatures from these DSC curves are listed for representative formulations in Table 3 and for the remaining formulations in Table S2. Notably, the Si2-20 %-CEL had an exotherm peak at 103 °C corresponding to crystallization of amorphous CEL material, followed by an endotherm melting peak of crystalline material at 159 °C. This is similar to literature observations of amorphous CEL (Wang et al., 2014) and indicates amorphous precipitation of CEL inside the pores of the cCVD Si2 particles. This was the only sample with an evident recrystallization peak. Such exotherm events can be challenging to identify, particularly for samples with low API mass load, for instance the 5 % loaded particle formulations. But other signs of non-crystalline, polymorph or molecularly adsorbed form of the drug are reduced melting enthalpies, reduction in melting temperatures or absence of endotherm melting peaks (Wang et al., 2014; Riikonen et al., 2015; Wang et al., 2010). This was for instance seen for Si1- and Si2-5 %-CEL, Si1-20 %-CEL, Si2-20 %-PHT, Si1- and Si2-20 %-GRI, Si1- and Si2-5 %-NAP and Si2-20 %-NAP. The corresponding physical mixtures showed a clear endothermic peak at the melting temperature, showing that the API contents of these samples were above the detection threshold for the instrument. Virtually no melting peak was seen for both the 5 % physical mixture and 5 % loaded samples for PHT, GRI and DCF samples. These samples were likely under the instrument's detection limit, and therefore gives little information about the solid form of the drugs. A melting peak was visible for the 20 % physical mixtures, except for DCF. A smaller endotherm melting peak, however, was observed for Si2-20 %-DCF compared to Si1-20 %-DCF. A shift of the onset/peak temperature, as was seen for some formulations, compared to the free API, could indicate a change in API crystal structure. Metastable crystalline polymorphs, for instance, have lower melting points than the most stable crystalline structure (Aulton, 2007). This can range from only a few degrees to 15–30 °C lower for different (polymorph) crystal forms (Lu et al., 2006; Pireddu et al., 2015). A polymorph form of NAP has even been reported with melting temperature as low as 76 °C (Song and Sohn, 2011). The CD raw materials, HPCD and SBCD, showed no sharp peaks but both had broad halo endotherm events around 100 °C which is typically seen for water content in hydrophilic samples (data not shown) (Wang et al., 2010). The average water contents were measured to 6 wt % for HPCD and 11 wt% for SBCD. The CD-API complexes showed similar broad peaks/halos to the CD raw material along with distinct melting peaks for the corresponding API. The API melting peaks were less clear or virtually not visible for the Si1-HPCD-API and Si1-SBCD-API samples.

3.2. Drug release of neutral drugs

The release data from the CEL-loaded Si1 and Si2 particle formulations are seen in Fig. 2a. Free CEL had a very slow dissolution with a maximum of 5 % dissolved after 4 h, whereas the loaded particles had a faster and higher release with 16 % released from Si2-5 %-CEL after 4 h, corresponding to a 3-fold improvement. There was a big difference between the Si1-5 %-CEL and Si1-20 %-CEL particles, with the former giving significantly higher release until 4 h. For the Si2 particles, the Si2-20 %-CEL released slower (significantly different until 30 min) but eventually to nearly the same extent as Si2-5 %-CEL. After 8–24 h, the Si1- and Si2-5 %-CEL formulations gave a decrease in %CEL released, approaching the level of free CEL. Using about a third of the amount of Si1- and Si2-5 %-CEL in the same release setup gave a similar initial fast release curve up to 2 h, without decreasing concentrations, and the maximum released after 24 h was 16–18 % (see Figure S9).

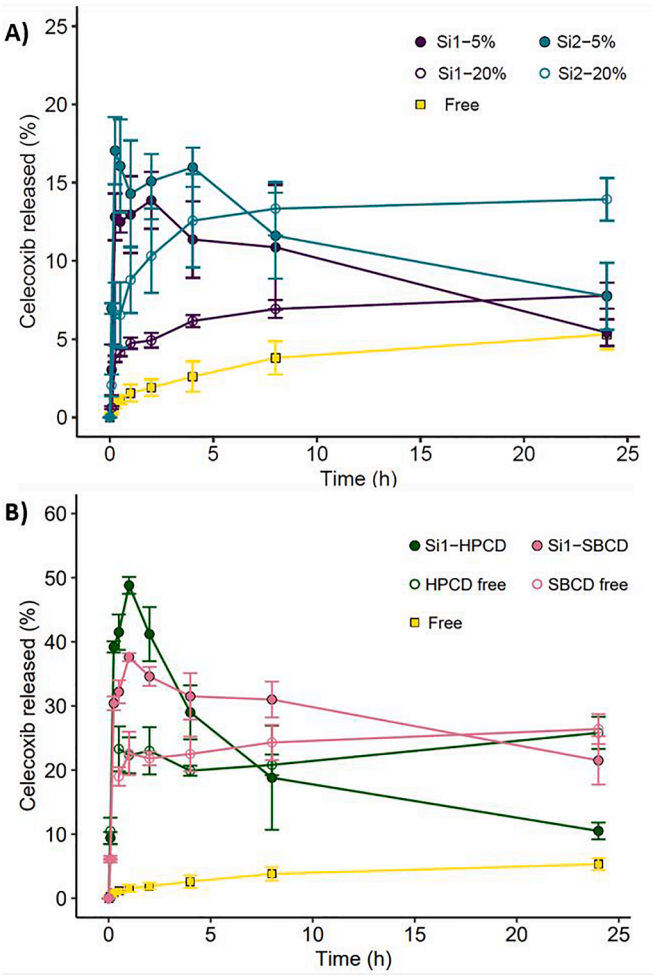


Fig. 2. Release curves of celecoxib (CEL), free CEL or CEL loaded into the Si1 and Si2 particles, in pH 7.4 (a). Si1-5 %-CEL had significantly higher release than Si1-20 %-CEL until 4 h. Si2-5 %-CEL had significantly higher release than Si2-20 %-CEL until 30 min. Release curves of CEL-CD-complexes (HPCD and SBCD), free or loaded into the Si1 particles, in pH 7.4 (b). Release was significantly higher for all formulations at all time-points, compared to free CEL dissolution, except for Si1-5 % and −20 % and Si2-5 % at 24 h.

Fig. 2b shows that the dissolution rate of the free HPCD-CEL and SBCD-CEL, which followed each other over the 24 h, was higher than the free CEL but lower than the loaded complexes. CD complexing improved the dissolution to about 22 % after just one hour, whereas Si1-HPCD-CEL and Si1-SBCD-CEL formulations gave a maximum dissolution of 49 % and 38 % after one hour, respectively. This corresponds to nearly ten times the dissolved amounts from the free drug. Thus, one can claim that synergistic dissolution effects (more than additive) were seen when CDs and cCVD Si particles were combined (1 h), surpassing both CD complexation and loading into the particles alone. This is the first report of loading CD-complexed drug molecules in silicon nanoparticles, as far as the authors know, and encourages further exploration of this promising combination.

A gradual decrease in released concentration, however, was observed for the fastest releasing CEL formulations, Si1-5 %-CEL, Si2-5 %-CEL, Si1-HPCD-CEL and Si1-SBCD-CEL, over longer time (>1h) which was not seen for the 20 % loaded formulations or free CD counterparts. After 24 h, this seems to approach the free CEL concentration for the loaded CEL and HPCD-CEL complex, whereas the SBCD-CEL complex decreased slower. This observation of "decreasing release" may arise from saturated solutions and precipitation from dissolution of metastable forms. The solubility of CEL around pH 7 is so low that

quantification has proven challenging, given the disparate reported values varying between for instance 3–7 μg/ml at 37 °C (Paulson et al., 2001; Jo et al., 2018) and 5.6–6.1 μg/ml at 25 °C (Madan et al., 2020; Dolenc et al., 2009). The experiments conducted at concentrations of ~5 μg/ml, close to the saturation limit, experienced precipitation while the experiments done at concentrations of ~1.4 μg/ml (Figure S9) did not. Yet, the release curves show a steep incline in dissolved amounts in the former scenario, a strong "spring-effect". This can be explained by the presence of amorphous or polymorph forms in the formulations that can result in supersaturated solutions due to their rapid dissolution rates. This thermodynamically unstable solution would adjust to move back to the true solubility, and the stable crystal form would start to precipitate to eventually give concentrations of the true equilibrium solubility of free CEL (not CD complexed).

The release data from the PHT-loaded particle formulations in Fig. 3 shows that the loaded PHT had a faster dissolution rate and gave a higher total release than the free drug control, at least up to 8 h (significant for all formulations). The release was significantly faster from the Si2-5 %-PHT than the Si2-20 %-PHT formulation for the first 4 h. The corresponding data for Si1-formulations showed non-significant differences.

For GRI release, shown in Fig. 4, the Si1-5 %-GRI formulation was the only one giving a significantly faster release than dissolution of the free drug, from 1-4 h. The Si1-20 %-GRI had a very similar profile to the free drug and the Si2 GRI-loaded particles had a slightly slower release than the free drug dissolved (non-significant).

When CD-complexed, GRI gave a higher release curve significantly improving the amount released after 8 h from 54 % for free GRI to 73–75 % for HPCD-GRI and SBCD-GRI. When formulating the CD-GRIs into the Si particles, the same level of % released as the free CDs was achieved after 24 h, however, the release was significantly faster between 1–4 h.

3.3. Drug release of acidic drugs

Both free DCF and NAP had a very fast dissolution rate in our experimental setup at pH 7.4 and the release from Si1-5 %-DCF and −NAP formulations both had a similar fast profile, see Figure S10.

The dissolution of free DCF in pH 2.0, on the other hand, was very slow compared to pH 7.4, with a maximum of 8 % dissolved after 24 h,

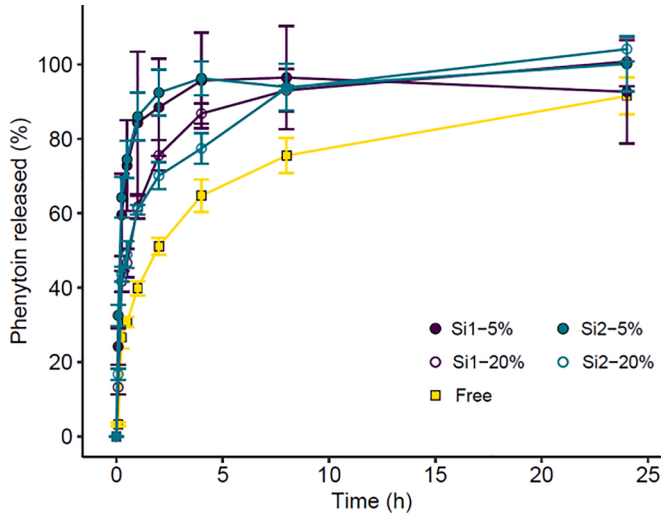


Fig. 3. Release curves of phenytoin (PHT), free PHT or PHT loaded into the Si1 and Si2 particles, in pH 7.4. All particle formulations had significantly higher release at all time-points, compared to free PHT dissolution, except for 8 h and 24 h for Si1-5 % and 24 h for Si1-20 % and Si2-5 %. Release was significantly faster from Si2-5 % than Si2-20 % for the first 4 h. Si1-5 % and Si1-20 % gave non-significant differences.

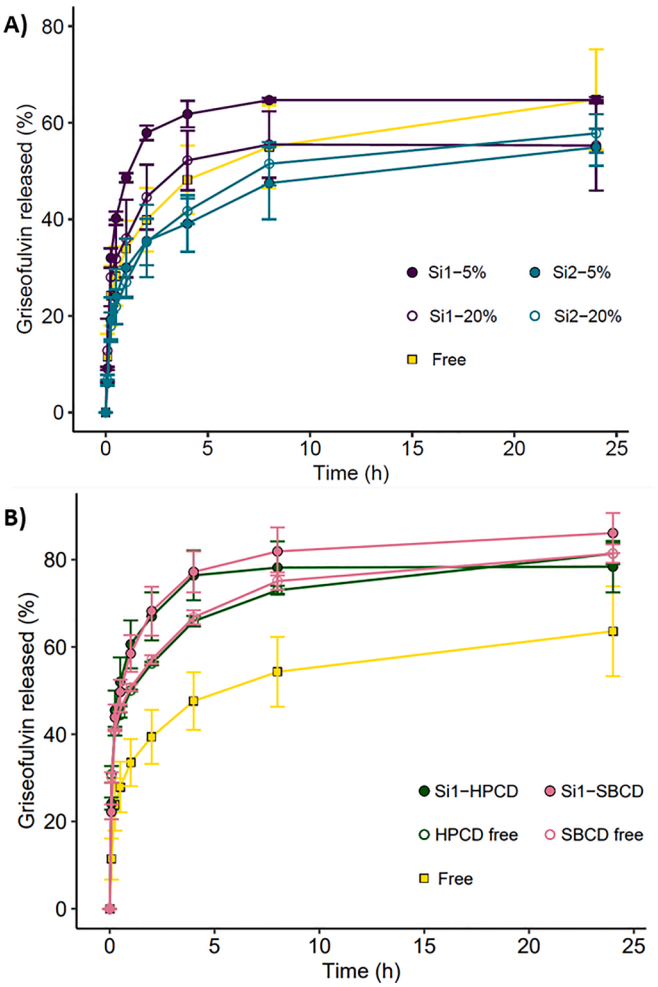


Fig. 4. Release curves of griseofulvin (GRI), free GRI or GRI loaded into the Si1 and Si2 particles, in pH 7.4 (a). Si1-5 % gave significantly faster release than free GRI 1–4 h. The other formulations did not give significantly faster release than free GRI. Release curves of GRI-CD-complexes (HPCD and SBCD), free or loaded into the Si1 particles, in pH 7.4 (b). All CD-formulations gave significantly higher release/dissolution than dissolution of free GRI at all time-points.

as shown in Fig. 5a. From the Si1-5 %-DCF formulation, the maximum released was increased to 20 %, whereas from the Si1-20 %-DCF formulation 11 % release was achieved. The release from the Si2-5 %-DCF and the Si2-20 %-DCF formulations was very similar with a maximum of 13–15 % released.

Fig. 5b shows the release curves of the CD-complexed DCF in pH 2.0. The free HPCD- and SBCD-DCF complexes both had a similar improved dissolution, compared to free DCF, gradually reaching 15 % and 13 % after 24 h, respectively. The Si1-SBCD-DCF release followed the free CD-DCFs for the first 8 h but gave a significantly higher release after 24 h (17 %). Si1-HPCD-DCF, on the other hand, had a rapid release up to 21 % after just 30 min and gave a total of 22 % after 24 h, which was non-significantly different from Si1-5 %-DCF. The significant improvements seen with the CEL-CD loaded particle formulations were therefore not observed for DCF, indicating a dependency on the API properties for achieving synergistic effect by the combination of Si particles and CD complexing.

Similar to DCF, free NAP had a slower dissolution in pH 2.0 (maximum 69 %) compared to pH 7.4, but the release was increased from all the particle formulations reaching >95 %. The release rate was significantly faster from both the Si1- and Si2-5 %-NAP compared to the Si1- and Si2-20 %-NAP formulations up to 4 h, but the same levels were reached after 8–24 h (see Fig. 6).

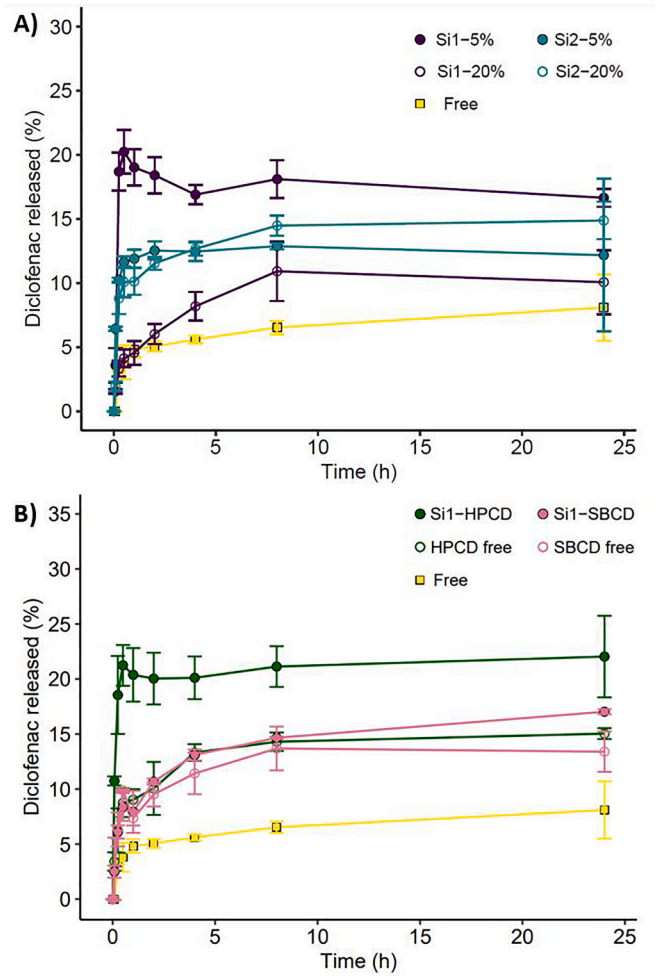


Fig. 5. Release curves of diclofenac (DCF), free DCF or DCF loaded into the Si1 and Si2 particles, in pH 2.0 (a). Release curves of DCF-CD-complexes (HPCD and SBCD), free or loaded into the Si1 particles, in pH 2.0 (b). All formulations gave significantly higher release than dissolution of free DCF at all time-points except for the Si1-20 % formulation (15 min-2 h, 24 h), Si2-5 % at 24 h, SBCD free at 5 min and HPCD free at 15 min.

3.4. General discussion of the formulations and mediums' impacts on the release results

The results obtained in this work have demonstrated the successful loading of 5 % and 20 % CEL, PHT, GRI, DCF and NAP into cCVD Si particles. Enhanced release rates were observed for most formulations compared to dissolution rates of the free drug counterparts. The sections above have presented and discussed the release results based on each drug substance separately. The following sections will compare the release results across the different drug substances and discuss how the drug dissolution varied significantly based on the formulations' characteristics, as well as the properties of the release environment such as the pH.

The effects of the cCVD Si particles and APIs properties

The intrinsic properties of the nanocarriers influenced both their drug loading and release performance. For most of the tested drugs, the Si2 particles gave higher release rates, while for certain formulations containing DCF and GRI the Si1 particles demonstrated slightly higher release. This variation may stem from minor differences in chemical composition that could affect drug affinities, but it was primarily attributed to the larger surface area and pore volume of Si2 particles. In the case of Si2 formulations with CEL and DCF, the release rates were less dependent on drug loading levels (5 % vs. 20 %) compared to Si1

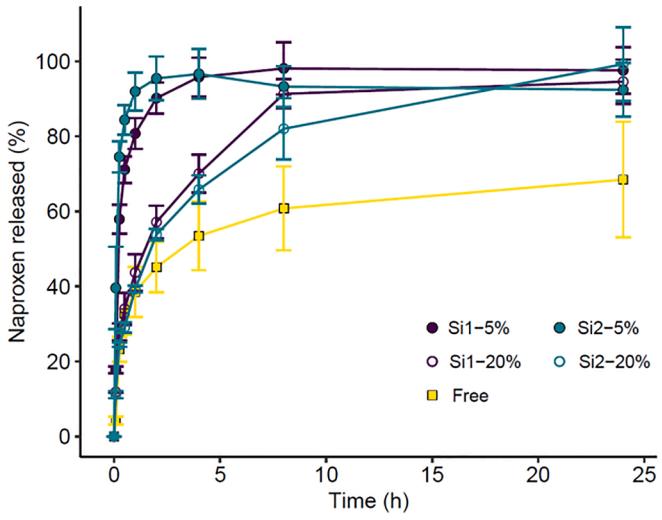


Fig. 6. Release curves of naproxen (NAP), free NAP or loaded NAP into the Si1 and Si2 particles, in pH 2.0. Si1- and Si2-5 % gave a significantly faster release than Si1- and Si2-20 %, respectively, up to 4 h. Significantly faster release was seen from the Si1- and Si2-5 % formulations, except for Si2-5 % at 24 h. The 20 % formulations did not give significantly different release at most time-points.

formulations. This was supported by the DSC data that showed amorphous exotherm recrystallization peaks or smaller endotherm melting peaks in the corresponding Si2 formulations. For the other APIs, a higher drug payload resulted in a slower release rate for both the Si1 and Si2 formulations. This was accompanied by a distinct melting peak in most of the 20 % loaded samples.

The theoretical pore filling capacity for CEL and NAP can be estimated, following the procedure described by Antonino *et al.* (Antonino et al., 2019) and Bavnhøj *et al.* (Bavnhøj et al., 2019), to 27 % and 23 % in Si2 particles and 19 % and 16 % in Si1 particles, respectively. These estimates suggest that Si1 particles have a drug loading capacity below 20 %, whereas Si2 particles can accommodate loads exceeding 20 %. Although these estimates were specific to the drug densities of CEL and NAP, they appear to align with experimental observations for CEL and DCF. Notable differences were also observed between 20 % loaded Si1 and Si2 samples when estimating crystallinity percentages based on their melting enthalpies (Table 3), in comparison to the 20 % physical mixtures with Si1 (Table S2), assuming that enthalpy is directly proportional to crystallinity and disregarding potential polymorphism and mixing effects. For the CEL loaded samples, this gave 82 % and 18 % crystallinity for Si1 and Si2, and for PHT load, this gave $>$ 100 % and 34 % crystallinity for Si1 and Si2 respectively. Smaller differences were seen for the other APIs. Additionally, most of the 20 % loaded formulations exhibited increased release rates compared to the free drug, despite showing distinct DSC melting peaks. The underlying mechanism for this is not entirely clear, but it may be due to an increased surface area available for dissolution or the presence of partially amorphous API up to the loading capacity. However, these hypotheses require further validation. The same loading technique was applied across all formulations in this study. To optimize the technique for each API, a systematic investigation could be conducted by varying solvent mixtures, temperature, pressure, or other parameters to maximize the proportion of amorphous forms.

The release performance of drug formulations is highly dependent on the interactions between the carrier and the drug payload. When an API is not covalently bound to its carrier, these interactions primarily involve ionic (electrostatic) or hydrophobic (van der Waals) interactions. Both types of intermolecular forces are believed to play a key role in drug-carrier interactions, thereby affecting the release characteristics, as depicted in Fig. 7.

The inherent properties of the model drug substances (Table 1)

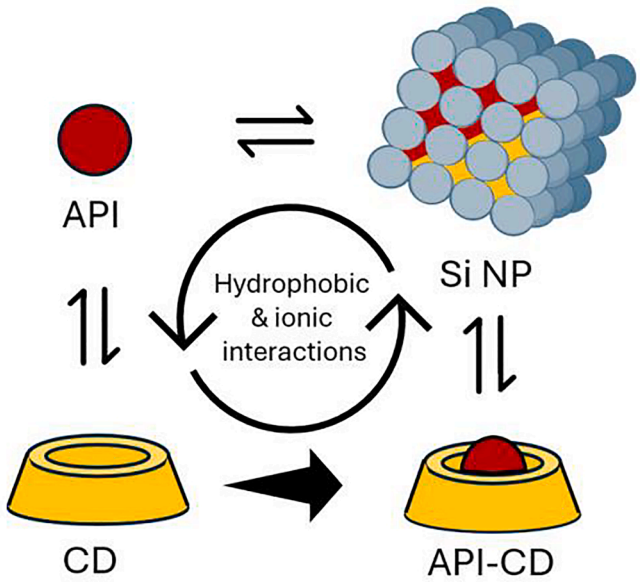


Fig. 7. Illustration of the interplay between API, CD and Si particles in the formulations. CD-complexation and loading of either API or API-CD are driven by both hydrophobic and ionic interactions, as the cCVD Si particles display negative zeta potential in water.

significantly influenced their release performance with the cCVD Si formulations. Notably, drugs with higher partition coefficients (hydrophobicity) and lower solubility, CEL and DCF (at pH 2.0), demonstrated marked improvements in dissolution when formulated with these particles. This may be due to a higher affinity (hydrophobic) of these drugs for the Si particle surface and a more effective loading into the pores, resulting in a greater proportion of amorphous material, as indicated by the DSC data. The five drugs examined herein were chosen as model compounds based on their chemical properties. Classified under BCS class II, most of these drugs exhibit low and/or variable oral bioavailability, highlighting the potential for enhancement through advanced formulation technologies. The cCVD Si particles may also offer a promising solution for improving the properties of new APIs under development, particularly those at risk of discontinuation due to poor dissolution rates or low bioavailability.

The effects of cyclodextrin complexation

The dissolution profiles of various API-CD combinations depend on the interplay between API inclusion into the CD cavity as well as the interactions between API-CD complex and the Si carrier. CD complexation of GRI, DCF and CEL enhanced their absolute solubilities, leading to an increased release from Si particles compared to Si-API formulations alone. CD complexes were made with CEL and DCF because the maximum level of release from the cCVD Si particle formulations were limited to 15–20 % despite achieving a 2–3-fold increase in dissolution compared to their free drug counterparts after 24 h. For GRI, the maximum achieved release from the Si particles was 65 %, similar to that of the free drug. The combination of CD-CEL with Si1 particles exhibited a more than additive effect at certain time points (<4 h), while CD-DCF showed only minor, non-significant improvements.

The type of CD used significantly influenced the release performance of the API-CD complexes. Previous studies have demonstrated enhanced dissolution of CEL when complexed with HPCD (Nagarsenker and Joshi, 2005) and SBCD (Rescifina et al., 2019), as well as DCF (Pose-Vilarnovo et al., 2003) and GRI (Veiga et al., 1998) when complexed with HPCD. SBCD has shown to be less toxic and more water-soluble than non-modified CDs (Das et al., 2019). These advantages could potentially exceed the toxicity and solubility of HPCD (Stella and Rajewski, 2020). In this study, HPCD combined with Si1 particles exhibited superior performance, compared to SBCD, for both DCF and CEL. The free API-CD complexes showed comparable performance across both CDs and all APIs tested. The lower performance of SBCD in some cases may be attributed to its negatively charged external substituents, which could decrease the affinity for loading into Si particles with a negative zeta potential. This ionic repulsion might reduce the efficacy of a combined system compared to the neutral HPCD. Additionally, the charge on SBCD could influence the inclusion of the API into the CD cavity (Okimoto et al., 1996). Therefore, the release performance of the API-CD loaded Si formulations depends on both the interactions between API and CD, and the interaction between the complexed API-CD and the Si particles (as illustrated in Fig. 7).

The peculiar observation of decreasing CEL concentrations seen after several hours from the fastest releasing CEL formulations, with and without CD, can potentially be attributed to metastable forms such as amorphous or crystal polymorphs. Supersaturated solutions arising from these metastable forms may persist long enough to enhance bioavailability of poorly soluble drugs (Raza et al., 2014). The reduced melting points observed in some formulations, such as Si1-20 %-CEL, −NAP and −DCF, Si2-20 %-NAP and −DCF, may also suggest polymorphism. However, mesoporous particles are unable to sustain a “parachute effect” that would maintain supersaturation levels. To mitigate API precipitation, particularly considering the water contents of 6–11 % in the CD raw materials, increasing the CD:API ratio beyond 1:1, for instance using 2:1, could be beneficial. However, this must be weighed against the loading capacity of the particles. The positive impact of polymorph forms on oral bioavailability has been documented in formulations of chloramphenicol palmitate (Aguiar et al., 1967); phenylbutazone (Pandit et al., 1984) and amobarbital (Kato and Kohketsu, 1981). Nonetheless, maintaining these polymorph or amorphous forms during storage poses a challenge (Aulton, 2007). Spatial confinement within mesoporous drug delivery materials could offer a favorable solution, as drug crystals are inhibited from forming, or potentially changing, due to the physical constraints imposed by pore size (Santos et al., 2011).

CD complexes were not prepared for PHT and NAP because the cCVD Si particles effectively addressed their slow dissolution rates, achieving 95 % release within 2–4 h compared to slower dissolution of free drug, which reached 65 % and 53 % after 4 h, respectively. Overall, we found this trend for the release rates of the studied formulations: Si1-HPCD > Si1-SBCD > free HPCD/SBCD > Si1 and Si2 loaded with 5 % API > Si1 and Si2 loaded with 20 % API > free API.

The effects of the release medium

For studying drug release kinetics, the release environment serves as another important variable, influenced by factors such as pH, salt content, temperature, and concentration. Herein, release testing was conducted at pH 7.4, and at pH 2.0 for the acidic drugs NAP and DCF. The release conditions were chosen for two reasons: to model *in vivo* conditions but also for simply studying the effects of the different parameters. In the intestines, where pH exceeds the acidic drugs’ pKa values, these drugs acquire a negative charge, slowing their uptake in these environments. It has been shown that the low-pH (<pKa) gut environment can facilitate uptake of acidic drugs (Schanker et al., 1957), due to the neutral charge at this pH, with a portion potentially absorbed via the gut lining. The paradox here lies in the fact that for solubility purposes, drugs should be in an ionized state, whereas for permeation, the non-ionized form is preferred. Elevated medium temperatures also augment drug solubility. Given that the release studies herein were conducted at room temperature, it is reasonable to anticipate higher dissolution rates *in vivo*. Considering the observed dissolution improvements even after 24 h in several of our experiments, an advantage also under physiological conditions can be anticipated. The salt contents in PBS can induce agglomeration of the Si particles (Johnsen et al., 2024), which can also affect release performance. Therefore, ultrasonication treatment was utilized to homogenize the samples in the beginning of each release experiment and reduce agglomeration effects.

Upon oral administration of a tablet, the local drug concentration in the GI tract can surpass the solubility in the limited volume available.

This might be the case for many BCS class II drugs as a higher dose is often used in response to poor bioavailability. Consequently, one might argue that release studies should mirror these conditions. Furthermore, continuous absorption into the bloodstream decreases the local drug concentration, forming a very different scenario than the somehow less relevant closed *in vitro* dissolution systems most often used. In standardized routine dissolution testing, 5 or 10-fold sink conditions are often used to make sure to avoid artificial saturation effects that can complicate data analysis (Siepmann and Siepmann, 2020), as is probably the explanations for decreasing concentration over time observed herein for some CEL formulations. Yet, the experiments herein were conducted with consistent drug concentrations for each API, allowing for direct comparisons (except the CEL data in Figure S9).

4. Conclusion

The novel aggregated silicon nanoparticles synthesized via centrifugal Chemical Vapor Deposition were shown to be versatile carriers capable of enhancing drug dissolution rates. The investigation of two types of cCVD Si particles and five different APIs, loaded at 5 % and 20 %, showed that parameters like API type, carrier properties and loading amount affected the release rates of the APIs. Observations of loaded drugs in an amorphous or non-crystalline state within certain particle formulations highlights the potential of these particles in improving the oral bioavailability of BCS class II drugs. Furthermore, the enhancements observed when loading CD-complexed drug molecules into the cCVD Si particles showed potential for further investigation of this novel combination with silicon nanocarriers. The formulation can thus be tailored for the needs of each API and their individual application. However, to fully realize the potential of this formulation strategy, further work is required to better understand the impact of various parameters during preparation of the formulations and dissolution testing.

Funding sources

This work was supported by the Research Council of Norway under the NANO2021 program, project number 313954.

CRediT authorship contribution statement

Hennie Marie Johnsen: Writing – review & editing, Writing – original draft, Visualization, Investigation, Formal analysis. **Werner Filtvedt:** Writing – review & editing, Conceptualization. **Jo Klaveness:** Writing – review & editing, Supervision, Methodology, Conceptualization. **Marianne Hiorth:** Writing – review & editing, Supervision, Project administration, Methodology.

Declaration of competing interest

The authors declare the following financial interests/personal relationships which may be considered as potential competing interests: Jo Klaveness, Werner Filtvedt and Hennie Marie Johnsen are inventors of a patent application with the title “Silicon particles for drug delivery”. The assignee of the patent application is Nacamed AS. Werner Filtvedt and Jo Klaveness have shares in Nacamed AS. Marianne Hiorth is an editor for the “Journal of Drug Delivery Science and Technology”.

Data availability

Data will be made available on request.

Appendix A. Supplementary data

Supplementary data to this article can be found online at https://doi.org/10.1016/j.ijpharm.2024.124809.

References

Aguiar, A.J., Krc Jr, J., Kinkel, A.W., Samyn, J.C., 1967. Effect of polymorphism on the absorption of chloramphenicol from chloramphenicol palmitate. J. Pharm. Sci. 56 (7), 847–853.
Antonino, R.S., Ruggiero, M., Song, Z., Nascimento, T.L., Lima, E.M., Bohr, A., Löbmann, K., 2019. Impact of drug loading in mesoporous silica-amorphous formulations on the physical stability of drugs with high recrystallization tendency. Int. J. Pharm.: X 1, 100026.
Aulton, M.E. (2007). Aulton's Pharmaceutics. Third edition. The design and manufacture of medicines. *Churchill Livingstone Elsivier*.
Bavnhøj, C.G., Knopp, M.M., Madsen, C.M., Löbmann, K., 2019. The role interplay between mesoporous silica pore volume and surface area and their effect on drug loading capacity. Int. J. Pharm.: X 1, 100008.
Chiarini, A., Tartarini, A., Fini, A., 1984. pH-Solubility relationship and partition coefficients for some anti-inflammatory arylaliphatic acids. Arch. Pharm. 317 (3), 268–273.
Das, O., Ghate, V.M., Lewis, S.A., 2019. Utility of sulfobutyl ether β-cyclodextrin inclusion complexes in drug delivery: a review. Indian J. Pharm. Sci. 81 (4).
Dolenc, A., Kristl, J., Baumgartner, S., Planinšek, O., 2009. Advantages of celecoxib nanosuspension formulation and transformation into tablets. Int. J. Pharm. 376 (1–2), 204–212.
Fahr, A., Liu, X., 2007. Drug delivery strategies for poorly water-soluble drugs. Expert Opin. Drug Deliv. 4 (4), 403–416.
GlobalData Healthcare (2018). Healthcare CPHI Experts: 90% of Current Pipeline APIs Are Poorly Soluble. Pharmaceutical technology, accessed 08 March 2024, https://www.pharmaceutical-technology.com/comment/cphi-experts-90-current-pipeline-apis-poorly-soluble/.
Inselman, A.L., Hansen, D.K. (2014). Phenytoin, Editor(s): Philip Wexler, *Encyclopedia of Toxicology* (Third Edition), Academic Press, 895-897.
Jacob, S., Nair, A.B., 2018. Cyclodextrin complexes: perspective from drug delivery and formulation. Drug Dev. Res. 79 (5), 201–217.
Jo, K., Cho, J.M., Lee, H., Kim, E.K., Kim, H.C., Kim, H., Lee, J., 2018. Enhancement of aqueous solubility and dissolution of celecoxib through phosphatidylcholine-based dispersion systems solidified with adsorbent carriers. Pharmaceutics 11 (1), 1.
Johnsen, H.M., Filtvedt, W., Hiorth, M., Klaveness, J., 2022. Silicon nanoparticles for oral administration of molecular hydrogen. Int. J. Pharm. 629, 122371.
Johnsen, H.M., Nasr, S.H., De Luna, R., Filtvedt, W., Sailor, M.J., Klaveness, J., Hiorth, M., 2024. Stable “snow lantern-like” aggregates of silicon nanoparticles suitable as a drug delivery platform. Nanoscale 16 (20), 9899–9910.
Kato, Y., Kohketsu, M., 1981. Relationship between polymorphism and bioavailability of amobarbital in the rabbit. Chem. Pharm. Bull. 29 (1), 268–272.
Kirkengen, M., Sauar, E., Filtvedt, W. (2021). Predominantly amorphous silicon particles and use thereof as active anode material in secondary lithium ion batteries. Patent application: WO2021160824.
Lee, J., Um, H.J., Sailor, M.J., Kim, J., Jeong, H., Kim, D., 2024. Adaptive cavitation ultrasonication for large-scale preparation of porous silicon nanoparticles. ACS Appl. Nano Mater. 7 (8), 9460–9468.
Lehto, V.P., Salonen, J., Santos, H., Riikonen, J., 2013. Nanostructured silicon-based materials as a drug delivery system for water-insoluble drugs. Drug Delivery Strategies for Poorly Water-Soluble Drugs 477–508.
León-Reyes, M.R., Castañeda-Hernández, G., Ortiz, M.I., 2009. Pharmacokinetic of diclofenac in the presence and absence of glibenclamide in the rat. J. Pharm. Pharm. Sci. 12 (3), 280–287.
Lin, C.C., Magat, J., Chang, R., McGlotten, J., Symchowicz, S., 1973. Absorption, metabolism and excretion of 14C-griseofulvin in man. J. Pharmacol. Exp. Ther. 187 (2), 415–422.
Loftsson, T., Brewster, M.E., 2010. Pharmaceutical applications of cyclodextrins: basic science and product development. J. Pharm. Pharmacol. 62 (11), 1607–1621.
Lu, G.W., Hawley, M., Smith, M., Geiger, B.M., Pfund, W., 2006. Characterization of a novel polymorphic form of celecoxib. J. Pharm. Sci. 95 (2), 305–317.
Madan, J.R., Ansari, I.N., Dua, K., Awasthi, R., 2020. Formulation and in vitro evaluation of casein nanoparticles as carrier for celecoxib. Adv. Pharm. Bull. 10 (3), 408.
Mura, P., 2020. Advantages of the combined use of cyclodextrins and nanocarriers in drug delivery: a review. Int. J. Pharm. 579, 119181.
Nagarsenker, M.S., Joshi, M.S., 2005. Celecoxib-cyclodextrin systems: characterization and evaluation of in vitro and in vivo advantage. Drug Dev. Ind. Pharm. 31 (2), 169–178.
Okimoto, K., Rajewski, R.A., Uekama, K., Jona, J.A., Stella, V.J., 1996. The interaction of charged and uncharged drugs with neutral (HP-β-CD) and anionically charged (SBE7-β-CD) β-cyclodextrins. Pharm. Res. 13, 256–264.
Pandit, J.K., Gupta, S.K., Gode, K.D., Mishra, B., 1984. Effect of crystal form on the oral absorption of phenylbutazone. Int. J. Pharm. 21 (1), 129–132.
Paulson, S.K., Vaughn, M.B., Jessen, S.M., Lawal, Y., Gresk, C.J., Yan, B., Karim, A., 2001. Pharmacokinetics of celecoxib after oral administration in dogs and humans: effect of food and site of absorption. J. Pharmacol. Exp. Ther. 297 (2), 638–645.
Pireddu, R., Sinico, C., Ennas, G., Marongiu, F., Muzzalupo, R., Lai, F., Fadda, A.M., 2015. Novel nanosized formulations of two diclofenac acid polymorphs to improve topical bioavailability. Eur. J. Pharm. Sci. 77, 208–215.
Pose-Vilarnovo, B., Rodríguez-Tenreiro Sánchez, C., Diéguez Moure, N., Vila-Jato, J.L., Torres-Labandeira, J.J., 2003. Effect of hydroxypropylmethyl cellulose on the complexation of diclofenac with cyclodextrins. J. Therm. Anal. Calorim. 73, 661–670.
Raza, K., Kumar, P., Ratan, S., Malik, R., Arora, S., 2014. Polymorphism: The phenomenon affecting the performance of drugs. SOJ Pharm. Pharm. Sci. 1 (10).

Rescifina, A., Surdo, E., Cardile, V., Avola, R., Graziano, A.C.E., Stancanelli, R., Tommasini, R., Pistarà, V., Ventura, C.A., 2019. Gemcitabine anticancer activity enhancement by water soluble celecoxib/sulfobutyl ether-β-cyclodextrin inclusion complex. Carbohydr. Polym. 206, 792–800.
Riikonen, J., Correia, A., Kovalainen, M., Näkki, S., Lehtonen, M., Leppänen, J., Lehto, V. P., 2015. Systematic in vitro and in vivo study on porous silicon to improve the oral bioavailability of celecoxib. Biomaterials 52, 44–55.
Runkel, R.A., Kraft, K.S., Boost, G., Sevelius, H., Forchielli, E., Hill, R., Magoun, R., Szakacs, J.B., Segre, E., 1972. Naproxen oral absorption characteristics. Chem. Pharm. Bull. 20, 1457–1466.
Salonen, J., Laitinen, L., Kaukonen, A.M., Tuura, J., Björkqvist, M., Heikkilä, T., Lehto, V. P., 2005. Mesoporous silicon microparticles for oral drug delivery: loading and release of five model drugs. J. Control. Release 108 (2–3), 362–374.
Samineni, R., Chimakurthy, J., Konidala, S., 2022. Emerging role of biopharmaceutical classification and biopharmaceutical drug disposition system in dosage form development: a systematic review. Turk. J. Pharm. Sci. 19 (6), 706.
Santos, H.A., Salonen, J., Bimbo, L.M., Lehto, V.P., Peltonen, L., Hirvonen, J., 2011. Mesoporous materials as controlled drug delivery formulations. J. Drug Delivery Sci. Technol. 21 (2), 139–155.
Schanker, L.S., Shore, P.A., Brodie, B.B., Hogben, C.A.M., 1957. Absorption of drugs from the stomach I. The rat. J. Pharmacol. Exp. Ther. 120 (4), 528–539.
Siepmann, J., Siepmann, F., 2020. Sink conditions do not guarantee the absence of saturation effects. Int. J. Pharm. 577, 119009.
Song, J.S., Sohn, Y.T., 2011. Crystal forms of naproxen. Arch. Pharm. Res. 34, 87–90.
Stella, V.J., Rajewski, R.A., 2020. Sulfobutylether-β-cyclodextrin. Int. J. Pharm. 583, 119396.
Sun, D., Gao, W., Hu, H., Zhou, S., 2022. Why 90% of clinical drug development fails and how to improve it? Acta Pharm. Sin. B 12 (7), 3049–3062.
Veiga, M.D., Díaz, P.J., Ahsan, F., 1998. Interactions of griseofulvin with cyclodextrins in solid binary systems. J. Pharm. Sci. 87 (7), 891–900.
Wang, F., Hui, H., Barnes, T.J., Barnett, C., Prestidge, C.A., 2010. Oxidized mesoporous silicon microparticles for improved oral delivery of poorly soluble drugs. Mol. Pharm. 7 (1), 227–236.
Wang, F., Barnes, T.J., Prestidge, C.A., 2014. Celecoxib confinement within mesoporous silicon for enhanced oral bioavailability. Open Mater. Sci. 1 (1).